

# Using magnetostriction to measure the spin-spin correlation function and magnetoelastic coupling in the quantum magnet $\text{NiCl}_2\text{-4SC}(\text{NH}_2)_2$

V. S. Zapf<sup>1</sup>, V. F. Correa,<sup>2,†</sup> P. Sengupta,<sup>1,3</sup> C. D. Batista,<sup>3</sup> M. Tsukamoto,<sup>4</sup>, N. Kawashima,<sup>4</sup> P. Egan,<sup>5</sup> C. Pantea,<sup>1</sup> A. Migliori,<sup>1</sup> J. B. Betts,<sup>1</sup> M. Jaime,<sup>1</sup> A. Paduan-Filho<sup>6</sup>

<sup>1</sup>National High Magnetic Field Laboratory (NHMFL),

Los Alamos National Lab (LANL), Los Alamos, NM

<sup>2</sup>NHMFL, Tallahassee, Florida

<sup>3</sup>Condensed Matter and Thermal Physics, LANL, Los Alamos, NM

<sup>4</sup>Institute for Solid State Physics,

University of Tokyo, Kashiwa, Chiba, Japan

<sup>5</sup>Oklahoma State University, Stillwater, OK

<sup>6</sup>Instituto de Física, Universidade de Sao Paulo, Brazil

<sup>†</sup> Now at Comisión Nacional de Energía Atómica,

Centro Atómico Bariloche, 8400 S. C. de Bariloche, Argentina

(Dated: October 29, 2018)

We report a method for determining the spatial dependence of the magnetic exchange coupling,  $dJ/dr$ , from magnetostriction measurements of a quantum magnet. The organic Ni  $S = 1$  system  $\text{NiCl}_2\text{-4SC}(\text{NH}_2)_2$  exhibits lattice distortions in response to field-induced canted antiferromagnetism between  $H_{c1} = 2.1$  T and  $H_{c2} = 12.6$  T. We are able to model the magnetostriction in terms of uniaxial stress on the sample created by magnetic interactions between neighboring Ni atoms along the c-axis. The uniaxial strain is equal to  $(1/E)dJ_c/dx_c\langle S_{\mathbf{r}} \cdot S_{\mathbf{r}+\mathbf{e}_c} \rangle$ , where  $E$ ,  $J_c$ ,  $x_c$  and  $\mathbf{e}_c$  are the Young's modulus, the nearest neighbor (NN) exchange coupling, the variable lattice parameter, and the relative vector between NN sites along the c-axis. We present magnetostriction data taken at 25 mK together with Quantum Monte Carlo calculations of the NN spin-spin correlation function that are in excellent agreement with each other. We have also measured Young's modulus using resonant ultrasound, and we can thus extract  $dJ_c/dx_c = 2.5$  K/Å, yielding a total change in  $J_c$  between  $H_{c1}$  and  $H_{c2}$  of 5.5 mK or 0.25% in response to an 0.022% change in length of the sample.

PACS numbers:

Keywords:

In many insulating magnets, the magnetic coupling is caused by superexchange interactions created when atomic or molecular orbitals overlap. Since the radial dependence of the orbital wave functions can be quite steep, the overlap integrals and the resulting exchange coupling  $J$  depend strongly on the interatomic bond lengths  $r$ . Past experiments have probed dependence of  $J$  on  $r$  using hydrostatic pressure or chemical substitution to vary the bond length, and Raman spectroscopy to measure  $J$ . These results were combined with high-intensity X-ray scattering measurements or elastic neutron scattering to determine the bond lengths.<sup>1,2,3,4</sup>

Here we demonstrate a simple and novel approach to investigating the spatial dependence of the superexchange interaction in the quantum magnet  $\text{NiCl}_2\text{-4SC}(\text{NH}_2)_2$  (DTN). We use applied magnetic fields to create an effective pressure and measure the response of the soft organic lattice via magnetostriction. The  $S = 1$  Ni ions in DTN form a body-centered tetragonal structure<sup>5</sup> shown in Fig. 1. The dominant magnetic superexchange interaction  $J_c = 2.2$  K is antiferromagnetic (AFM) and occurs along linear Ni-Cl-Cl-Ni bonds in the tetragonal c-axis.<sup>6,7</sup> Along the a-axis,  $J_a = 0.18$  K is an order of magnitude smaller and no diagonal or next-nearest neighbor couplings have been found within the resolution of inelastic neutron scattering measurements.<sup>6</sup> We thus treat this compound as a 1D system of Ni-Cl-Cl-Ni chains only weakly coupled in the a-b plane. Because  $J_c$  is sensitive to the Ni inter-ion bond lengths, a magnetic stress is created between adjacent Ni spins along the c-axis. This stress depends on the

relative orientation of the two spins, e.g. on the NN spin-spin correlation function  $\langle S_{\mathbf{r}} \cdot S_{\mathbf{r}+\mathbf{e}_c} \rangle$ .

In DTN, the NN spin-spin correlation function varies strongly with magnetic field. DTN exhibits AFM order for applied fields along the c-axis between  $H_{c1} = 2.1$  T and  $H_{c2} = 12.6$  T and with a maximum Néel temperature of  $T_N = 1.2$  K, as shown in the phase diagram in Fig. 2. The AFM order is confined to the a-b plane at  $H_{c1}$ . However, as the field is increased from  $H_{c1}$  to  $H_{c2}$ , the spins cant along the c-axis and finally saturate for  $H > H_{c2}$ . This is illustrated in the magnetization vs field curve shown in Fig. 2.

The lack of magnetic order at zero field is due to a strong easy-plane uniaxial anisotropy that creates a splitting  $D$  at zero field between the  $S_z = 0$  ground state and the  $S_z = \pm 1$  excited states of the Ni ion. In applied fields parallel to the tetragonal c-axis, the Zeeman effect then lowers the  $S_z = -1$  state until it becomes degenerate with the  $S_z = 0$  state, resulting in a magnetic ground state and AFM order below the Néel temperature.<sup>7</sup> Since the  $S_z = -1$  state is broadened by AFM dispersion, the region of overlap between  $S_z = -1$  and  $S_z = 0$  extends from  $H_{c1} = 2.1$  T up to  $H_{c2} = 12.6$  T.

Here we show that the bare NN spin-spin correlation function can be directly proportional to the c-axis magnetostriction. Since all the terms in the magnetic Hamiltonian of this compound have been measured, we can calculate  $\langle S_{\mathbf{r}} \cdot S_{\mathbf{r}+\mathbf{e}_c} \rangle$  using Quantum Monte Carlo simulations to predict the magnetostriction response as a function of the applied magnetic field. By combining these results with resonant ultrasound

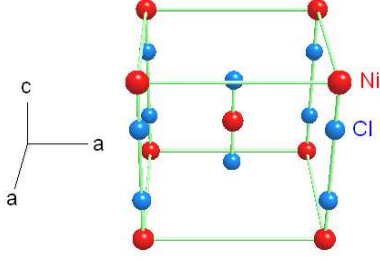


FIG. 1: Unit cell of tetragonal  $\text{NiCl}_2\text{-4SC(NH}_2)_2$  showing Ni (red) and Cl (blue) atoms. The thiourea molecules have been omitted for clarity.

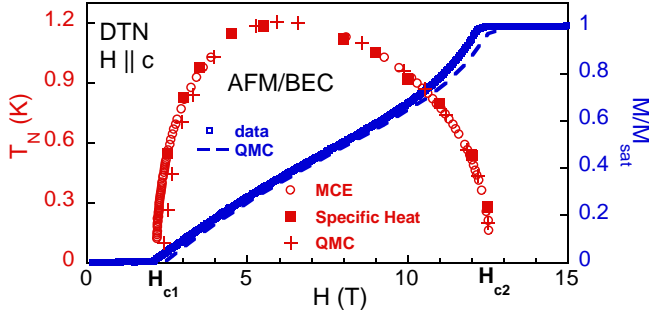


FIG. 2: Temperature  $T$  - Magnetic field  $H$  phase diagram for  $H||c$  determined from specific heat and magnetocaloric effect (MCE) data, together with the result of Quantum Monte Carlo (QMC) simulations.<sup>6,7</sup> The magnetization vs field measured at 16 mK and calculated from QMC is overlaid onto the phase diagram.<sup>8</sup>

spectroscopy to determine the elastic moduli, we are also able to extract the leading linear term in the spatial dependence of the exchange interaction  $J_c(r)$  along the tetragonal  $c$ -axis.

We first present magnetostriction measurements that were performed on single crystals of DTN down to 25 mK in a 20 T magnet at the National High Magnetic Field Laboratory in Tallahassee, FL, as described in Ref. 9. The magnetostriction as a function of  $H$  for  $H||c$  is shown in Fig. 3 for both the  $a$  and  $c$ -axes of the crystal. The  $c$ -axis magnetostriction  $\Delta L_c/L_c$  shows sharp shoulders at the boundaries of the ordered state at  $H_{c1}$  and  $H_{c2}$ , and nonmonotonic behavior in between. The net difference between the  $c$ -axis lattice parameter at  $H_{c1}$  and  $H_{c2}$  is 0.022%. The nonmonotonic behavior of the magnetostriction contrasts with the roughly linear dependence of the magnetization  $M(H)$  in the region of AFM order between  $H_{c1}$  and  $H_{c2}$ , as shown in Fig. 2. It also contrasts with the magnetostriction observed in the Cu dimer spin gap system  $\text{KCuCl}_3$ , in which the magnetostriction closely tracks the magnetization.<sup>10</sup>

The  $a$ -axis lattice parameter decreases monotonically by an amount that is an order of magnitude smaller than the change in the  $c$ -axis parameter, reflecting the fact that  $J_a \ll J_c$ . The  $a$ -axis behavior is more difficult to explain since the exchange interaction is mediated by an unknown and likely convoluted path, and because the  $a$ -axis is subject to significant Poisson

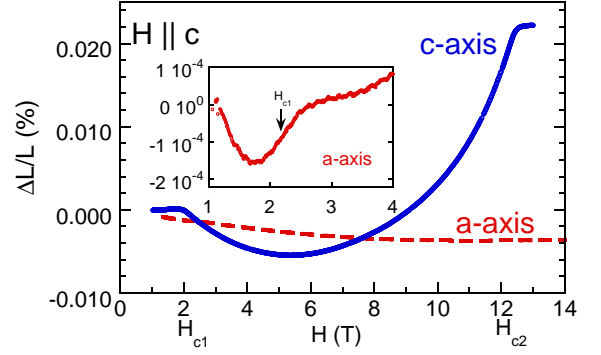


FIG. 3: Normalized percentage length change  $\% \Delta L/L$  as a function of magnetic field measured along the crystallographic  $c$ -axis (solid blue lines) and  $a$ -axis (dashed red lines). The data is taken at  $T = 25$  mK with the magnetic field applied along the  $c$ -axis. The inset shows the feature at  $H_{c1}$  in  $\% \Delta L_a/L_a$  in greater detail, and a straight line has been subtracted from the inset data for clarity.

forces from the larger  $c$ -axis distortion.

We thus focus on the  $c$ -axis magnetostriction and we suggest a straightforward explanation for its nonmonotonic field-dependence between  $H_{c1}$  and  $H_{c2}$ . The canted AFM order results in two competing forces on the  $c$ -axis of the lattice. Near  $H_{c1}$ , the Ni spins order antiferromagnetically, thus creating an attractive force. By reducing the  $c$ -axis lattice parameter, the system can increase  $J_c$ , and thereby lower the energy of the antiferromagnetically aligned spins. However, with increasing field the spins cant, resulting in a ferromagnetic component to the order. The ferromagnetic component stretches the lattice, thereby reducing  $J_c$ . Once the magnetic field exceeds  $\sim 5.5$  T, the ferromagnetic component wins and the lattice expands.

We now test this model by calculating the expected  $c$ -axis magnetostriction. The energy density of the system can be written as the sum of magnetic and lattice components,  $\epsilon = \epsilon_e + \epsilon_m$ , with

$$\begin{aligned} \epsilon_e &= \frac{1}{2} E \left( \frac{x_c - c_0}{c} \right)^2 \\ \epsilon_m &= \frac{2}{N a^2 c} \langle \mathcal{H}_m \rangle \end{aligned} \quad (1)$$

Here  $a$  and  $c$  are the lattice parameters at zero field.  $E$  is Young's modulus along the  $c$ -axis and  $N$  is the total number of Ni sites. The factor of 2 is required because there are two Ni atoms per unit cell of volume  $a^2 c$ . The variable  $c_0$  is the value of the lattice parameter along the  $c$ -axis in the absence of magnetic interactions and external pressure. The variable  $x_c$  is the new value of the lattice parameter when the magnetic interactions are included. We have neglected the effect of  $a$ -axis strain inducing changes in the  $c$ -axis via the Poisson ratio since it is a 1 % effect.

The magnetic Hamiltonian  $\mathcal{H}_m$  is:

$$\mathcal{H}_m = \sum_{\mathbf{r}, \nu} J_\nu \mathbf{S}_{\mathbf{r}} \cdot \mathbf{S}_{\mathbf{r}+\mathbf{e}_\nu} + \sum_{\mathbf{r}} [D(S_{\mathbf{r}}^z)^2 - g\mu_B H S_{\mathbf{r}}^z], \quad (2)$$

where  $e_\nu = \{a\hat{x}, b\hat{y}, c\hat{z}\}$  are the relative vectors between NN Ni ions along the a, b and c-axis respectively. In this Hamiltonian, the magnitude of the various parameters  $D$ ,  $J_a$ ,  $J_c$ , and  $g$  have been measured experimentally via ESR and neutron diffraction in combination with Quantum Monte Carlo simulations.<sup>6,7</sup>

We can now obtain the value of  $x_c$  as a function of magnetic field by minimizing the total energy with respect to  $x_c$ :

$$\partial_{x_c} \epsilon = \frac{E}{c^2} (x_c - x_o) + \partial_{x_c} \epsilon_m = 0. \quad (3)$$

We assume that the only term in  $\mathcal{H}_m$  that depends on  $x_c$  is the AFM Heisenberg coupling along the c-axis. The single-ion anisotropy  $D$  typically has a much smaller dependence on  $x_c$ . In addition, since the temperature at which the magnetostriction measurements were performed (25 mK) is much lower than any characteristic energy of the system, we will assume that  $T = 0$  K. Under these conditions we obtain:

$$\partial_{x_c} \epsilon_m = \frac{2}{a^2 c} \partial_{x_c} J|_{x_c=c} \langle \mathbf{S}_r \cdot \mathbf{S}_{r+e_c} \rangle. \quad (4)$$

In Eq. 4 we have applied the Hellman–Feynman and assumed that  $\partial_{x_c} J \simeq \partial_{x_c} J|_{x_c=c}$  because the relative distortion is very small. Substituting into Eq. (3) we find that:

$$\frac{E}{c^2} (x_c - x_o) + \frac{1}{a^2 c} \partial_{x_c} J|_{x_c=c} \langle \mathbf{S}_r \cdot \mathbf{S}_{r+e_c} \rangle = 0. \quad (5)$$

We know that  $x_c = c$  for  $H = 0$  and thus,

$$\frac{E}{c^2} (c - x_o) + \frac{1}{a^2 c} \partial_{x_c} J|_{x_c=c} \langle \mathbf{S}_r \cdot \mathbf{S}_{r+e_c} \rangle_{H=0} = 0, \quad (6)$$

where  $\langle \mathbf{S}_r \cdot \mathbf{S}_{r+e_c} \rangle_{H=0}$  indicates that the mean value is computed for a field  $H = 0$ . By taking the difference between Eqs. 5 and 6 we obtain:

$$\frac{\Delta L}{L} = -\frac{\partial_{x_c} J|_{x_c=c}}{a^2 E} [\langle \mathbf{S}_r \cdot \mathbf{S}_{r+e_c} \rangle_{H=0} - \langle \mathbf{S}_r \cdot \mathbf{S}_{r+e_c} \rangle_H], \quad (7)$$

where  $\Delta L/L = (x_c - c)/c$ . Thus our measured c-axis magnetostriction is proportional to the NN spin-spin correlation function with a proportionality constant of

$$\kappa = \frac{1}{a^2 E} \partial_{x_c} J|_{x_c=c}. \quad (8)$$

We can therefore model the experimental magnetostriction data with the parameter  $\kappa$  as the only fitting parameter. We have determined the NN spin-spin correlation function using Quantum Monte Carlo simulations on a  $8 \times 8 \times 24$  lattice and the parameters:  $J_c = 2.2$  K,  $J_a = 0.18$  K, and  $D = 8.6$  K.<sup>7</sup> The results of our model are shown in comparison with the measured magnetostriction in Fig. 4, with  $\kappa = 1.00 \times 10^{-5}$ . The agreement between theory and experiment is very good and confirms our hypothesis that the spatial dependence of  $D$  is much smaller than the spatial dependence of  $J$  and can thus be neglected. This is to be expected since  $J$  results from the overlap integral between adjacent molecular wave functions, which can have large radial

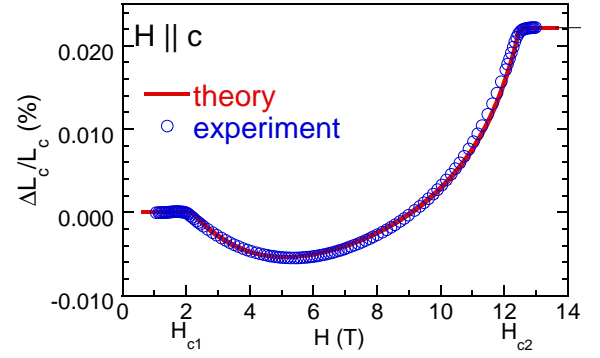


FIG. 4: Comparison of experimental c-axis magnetostriction data as a function of  $H$  for  $H||c$  with the model described in the text.

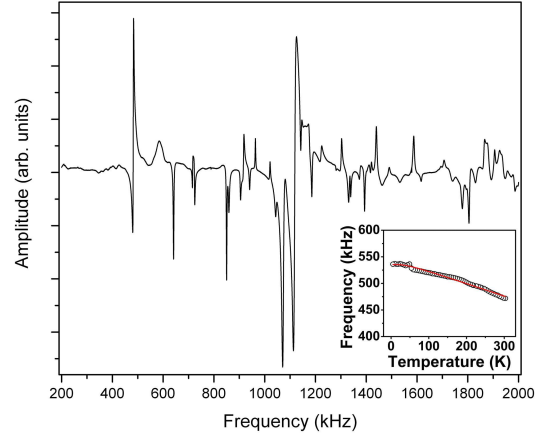


FIG. 5: Mechanical resonances of DTN at room temperature. Inset: Temperature-dependence of the major peak near 500 kHz between 5 K and 300 K. The line is a fit to the usual Einstein oscillator model equation<sup>11</sup> and used to extrapolate the resonance to 0 K.

dependencies with high power-laws, whereas  $D$  depends on crystalline electric fields that change more weakly with lattice distortions. For instance, previous experimental and theoretical works on other compounds have modelled the spatial dependence of superexchange interactions as a power-law  $J(r) = br^{-n}$  where  $r$  is the relevant spacing between magnetic ions. Values for the exponent  $n$  of 10-14 have been reported for metal halides,<sup>2,3</sup> and 2-7 for cuprates.<sup>14</sup> In this work, we are determining the leading linear term in the expansion of  $J(r)$ , e.g.  $\partial_r J \approx -nJ/r$ . We have neglected higher order terms because the relative change of the lattice parameter  $c$  that results from the magnetic stress is always smaller than 0.03% as shown in Fig.3.

We take our analysis one step further and quantitatively determine the spatial dependence of the AFM exchange interaction  $dJ_c/dx_c$  from Eq. 8. The lattice parameters  $a = 9.558$  Å and  $c = 8.981$  Å are known from published X-ray diffraction measurements at 110 K.<sup>5</sup> That leaves Young's modulus  $E$  as the remaining quantity to be determined before we can extract  $dJ_c/dx_c$ .

Thus, we have also measured Young's modulus using Resonant Ultrasound Spectroscopy (RUS) between 300 K and 5 K.<sup>12,13</sup> Mechanical resonances of a roughly cube-shaped single crystal of DTN were determined at zero field in a He-cooled Oxford Instruments flow-cryostat. The six independent elastic moduli were determined between 300 K and 200 K and their values at room temperature are shown in Table I.

For lower temperatures, determination of all of the resonances used in the fitting procedure became ambiguous. However, two good resonances could be identified down to 5 K and based on the temperature dependencies of these resonances, we extrapolated the value of Young's Modulus to 0 K. Young's modulus  $E$  in a tetragonal crystal is given by:

$$E_{33} = C_{33} - \frac{2C_{13}^2}{C_{11} + C_{12}}, \quad (9)$$

yielding  $E = 7.5 \pm 0.7$  GPa at 0 K.

Now we can use equation (9) to calculate  $\partial_x J|_{x=x_0} = dJ_c/dx_c = 2.5$  K/Å, yielding a total change in  $J_c$  between  $H_{c1}$  and  $H_{c2}$  of 5.5 mK or 0.25%. This in turn results in a 0.1% shift in  $H_{c2}$  relative to its value in the absence of magnetostriction effects. The dominant uncertainty in these calculations comes from the 10% error bar in estimating Young's modulus  $E$  due to the softness of the crystal.

Previous papers about DTN have assumed that  $J_c$  is constant when calculating the critical fields, the magnetization, and other field-dependent measurable quantities.<sup>6,7</sup> Since  $J_c$  only varies by 0.25%, these assumptions are quite reasonable and well within experimental error. An open question remains, however, whether the symmetry of the crystal is affected by the magnetostriction. DTN has previously attracted interest because the field-induced phase transition at  $H_{c1}$  likely belongs to the universality class of Bose-Einstein Condensation (BEC).<sup>6</sup> The tetragonal symmetry of the lattice creates a necessary condition for conservation of the equilibrium number of bosons, and therefore structural deviations away from tetragonal crystal symmetry could disallow the Bose-Einstein Condensation picture. Since the magnetostriction effects occur gradually at fields above  $H_{c1}$ , the BEC picture would hold right at  $H_{c1}$  as reported,<sup>6</sup> but become less valid at high fields as the structure becomes increasingly distorted. This possibility is currently being further investigated via elastic neutron diffraction and ESR measurements.

It has been suggested that sound attenuation studies, which probe magnon-phonon coupling, are another means of prob-

ing the magnitude of  $J(r)$ .<sup>14</sup> However, as demonstrated in measurements of a similar antiferromagnetic quantum magnet  $\text{TiCuCl}_3$ ,<sup>15</sup> the wave vector  $k$  of the probing phonons is vanishingly small compared to the wave vector of the magnons, and thus the contribution of  $J(r)$  to the magnon-phonon coupling is negligible compared to the contribution of  $D(r)$ .

To our knowledge, the superexchange interaction in Ni-Cl-Cl-Ni chains has not been previously investigated experimentally or theoretically. For DTN, we speculate that the Cl-Cl bond determines the magnitude of  $J$  along the Ni-Cl-Cl-Ni chains, since it is the weakest link, being nearly 2x longer than the Ni-Cl bond (4.1 Å vs 2.4 or 2.5 Å). Early X-ray scattering studies have also implied<sup>5</sup> that the lowest-energy lattice

TABLE I: Tetragonal elastic moduli of DTN at room temperature.

elastic moduli (GPa)	
$c_{11} = 26.1$	$c_{12} = 15.3$
$c_{33} = 14.2$	$c_{44} = 11.2$
$c_{23} = 12.4$	$c_{66} = 4.3$

vibrations consist of the  $\text{NiCl}_2\text{-4SC(NH}_2)_2$  molecule moving as a unit, thus supporting the idea that the Cl-Cl bonds that link adjacent molecules are more susceptible to pressure than the Ni-Cl bonds within a molecule.

In summary, we have measured magnetostriction of the organic quantum magnet  $\text{NiCl}_2\text{-4SC(NH}_2)_2$  and we have modelled the magnetostriction data by treating the compound as a 1-D magnetic system in which the strong dependence of the superexchange interaction on the bond lengths along the c-axis results in a magnetic stress. To our knowledge, this is the first work in which the NN spin-spin correlation function is shown to be directly proportional to an experimentally measurable quantity. It also presents a new and straightforward method for determining the spatial dependence of the exchange coupling over small distances.

### Acknowledgments

This work was supported by the DOE, the NSF, and Florida State University through the National High Magnetic Field Laboratory. A.P.F. acknowledges support from CNPq (Conselho Nacional de Desenvolvimento Científico e Tecnológico, Brazil). We would like to thank S. Haas and N. Harrison for stimulating discussions.

<sup>1</sup> M. C. Aronson, S. B. Dierker, B. S. Dennis, S.-W. Cheong, and Z. Fisk, Phys. Rev. B **44**, 4657 (1991).

<sup>2</sup> M. J. Massey, N. H. Chen, J. W. Allen, and R. Merlin, Phys. Rev. B **42**, 8776 (1990), and references therein.

<sup>3</sup> W. A. Harrison, *Electronic Structure and the Properties of Solids* (Freeman, San Francisco, 1980).

<sup>4</sup> S. L. Cooper, G. A. Thomas, A. J. Millis, P. E. Sulewski, J. Orenstein, D. H. Rapkine, S.-W. Cheong, and P. L. Trevor, Phys. Rev. B **42**, 10785 (1990).

<sup>5</sup> A. Lopez-Castro and M. R. Truter, J. Chem. Soc. p. 1309 (1963).

<sup>6</sup> V. S. Zapf, D. Zocco, B. R. Hansen, M. Jaime, N. Harrison, C. D. Batista, M. Kenzelmann, C. Niedermayer, A. Lacerda, and A. Paduan-Filho, Phys. Rev. Lett. **96**, 077204 (2006).

<sup>7</sup> S. Zvyagin, J. Wosnitza, C. D. Batista, M. Tsukamoto, N. Kawashima, J. Krzystek, V. S. Zapf, M. Jaime, N. F. O. Jr., and A. Paduan-Filho, Phys. Rev. Lett. **98**, 047205 (2007).

<sup>8</sup> A. Paduan-Filho, X. Gratens, and N. F. O. Jr., Phys. Rev. B **69**, 020405(R) (2004).

- <sup>9</sup> V. S. Zapf, V. Correa, C. D. Batista, T. Murphy, E. D. Palm, M. Jaime, S. Tozer, A. Lacerda, and A. Paduan-Filho, *J. Appl. Phys.* **101**, 09E106 (2007).
- <sup>10</sup> Y. Sawai, S. Kimura, T. Takeuchi, K. Kindo, and H. Tanaka, *Prog. Theoretical Phys. Suppl.* **159**, 208 (2005).
- <sup>11</sup> Y. P. Varshni, *Phys. Rev. B* **2**, 3952 (1970).
- <sup>12</sup> A. Migliori and J. Sarrao, *Resonant Ultrasound Spectroscopy* (Wiley, New York, NY, 1997).
- <sup>13</sup> A. Migliori, J. Sarrao, W. Visscher, T. Bell, M. Lei, Z. Fisk, and R. Leisure, *Physica B* **183**, 1 (1993).
- <sup>14</sup> M. G. Cottam, *J. Phys. C: Solid State Phys.* **7**, 2901 (1974).
- <sup>15</sup> E. Y. Sherman, P. Lemmens, B. Busse, A. Oosawa, and H. Tanaka, *Phys. Rev. Lett.* **91**, 057201 (2003).